Energy Reports 12 (2024) 2498–2510

Contents lists available at ScienceDirect

Energy Reports

journal homepage: www.elsevier.com/locate/egyr

Review Article

Design and implementation of an autonomous device with an app to monitor the performance of photovoltaic panels

A. Ordoñez [a], J. Urbano [a], F. Mesa [b,*], M. Castañeda [c], S. Zapata [d], B. Quesada [e], O. García [a], A.J. Aristizábal [a]

[a] Universidad Jorge Tadeo Lozano, Bogotá, Colombia
[b] Fundación Universitaria Los Libertadores, Bogotá, Colombia
[c] Universidad Católica de Valparaíso, Valparaiso, Chile
[d] Universidad EIA, Envigado, Colombia
[e] Earth System Sciences Program, Faculty of Natural Sciences, Universidad del Rosario, Bogotá, Colombia

ARTICLE INFO

Keywords:
Solar Photovoltaics
PV monitoring
Solar Energy
Renewables
PV performance

ABSTRACT

Photovoltaics (PV) utilize sunlight to generate electricity, thus playing a crucial role in generating clean energy and decreasing carbon emissions. Simultaneously, these systems encourage self-sufficiency in energy production. Consequently, it becomes imperative to monitor the performance of photovoltaic systems as an essential method for assessing and confirming these advantages. Precise measurement and analysis of performance data offer researchers and industry experts valuable insights into system effectiveness, power generation trends, as well as their overall ecological influence. The significance of PV monitoring in ensuring and enhancing system performance is emphasized by the research conducted. The ability to collect and analyze real-time data enables operators to identify inefficient modules, as well as shading or other obstacles that could hinder energy production. Furthermore, monitoring systems enable early identification of potential malfunctions, which allows for timely maintenance and repair actions. Ultimately, these practices enhance overall energy generation while extending the longevity of PV installations. This paper presents the design and implementation of a portable electronic device to measure the I-V and P-V curves of photovoltaic panels. This instrument acquires solar radiation, ambient temperature, electric current, and voltage signals from a PV panel via a cellphone through a mobile application. The device, capable of real-time characterization of PV panels up to 20 A and 500 V, features a 240 MHz Tensilica LX6 dual-core processor and 4 MB of storage memory. Experimental tests were carried out in two different geographical locations in Colombia: the city of Puerto Carreño and the city of Bogotá. Among the main results, an efficiency of 13.29 % was obtained for solar radiation of 755.47 W/m^2 and a temperature of 29.60 °C for a monocrystalline PV panel of 405 W.

1. Introduction

Photovoltaic energy is inherently sustainable, producing electricity without direct greenhouse gas emissions or other harmful pollutants. It plays a vital role in mitigating climate change by reducing carbon dioxide (CO_2) emissions, thus contributing to global efforts to combat global warming. As a result, PV energy stands as a promising solution to achieve decentralized electricity, carbon neutrality and minimize the environmental footprint of electricity generation (Hosseini et al., 2023).

As the adoption of PV technology continues to increase worldwide, it is crucial to understand and address potential environmental concerns throughout the entire lifecycle of these renewable energy systems. Its necessary to identify and evaluate key environmental factors affecting the performance of photovoltaic panels (Jathar et al., 2023). There is a crucial need for accurate and reliable testing and performance evaluation of PV modules, providing valuable insights into their efficiency and behavior under varying environmental conditions. The PV industry encompasses the design and implementation of solar simulators, as well as automatic I-V curve acquisition systems, which play a pivotal role in streamlining the testing process and generating critical data for PV module evaluation (Piccoli Junior et al., 2023). One of the main problems of PV technology pertains to the need for a fast, efficient, and

* Corresponding author.
E-mail address: fredy.mesa@libertadores.edu.co (F. Mesa).

https://doi.org/10.1016/j.egyr.2024.07.062
Received 22 April 2024; Received in revised form 18 July 2024; Accepted 29 July 2024
Available online 27 August 2024

accurate method to characterize the current-voltage (I-V) curves of photovoltaic (PV) arrays. I-V curves are essential in evaluating the performance, efficiency, and health of PV arrays, as they provide crucial information about the electrical behavior of the system under different operating conditions. However, traditional methods of acquiring I-V curves can be time-consuming and impractical, especially when dealing with large-scale PV installations (Chen et al., 2020). When photovoltaic panels are subject to defects or malfunctions, the traditional I-V curve measurement methods prescribed by the IEC 60891 standard may lead to inaccurate or unreliable results. These defects can manifest in various forms, such as partial shading, hotspots, module degradation, or electrical mismatches within the PV panel. When conventional I-V curve measurement techniques are applied to defective panels, the resulting data may not represent the true electrical characteristics of the PV module (Li et al., 2021; Liu et al., 2021; Ma et al., 2020).

Various internal and external factors can lead to defects or malfunctions in photovoltaic panels, compromising their functionality and reducing their energy generation capacity. Full I-V characteristics provide a comprehensive understanding of the electrical behavior of the PV panel under different operating conditions, allowing for a more detailed fault analysis. PV researchers employ machine learning techniques to process and interpret the full I-V characteristics for fault diagnosis. Machine learning algorithms, such as support vector machines, decision trees, or neural networks, are trained with data from healthy and faulty photovoltaic panels to recognize patterns and correlations associated with specific faults (Ma et al., 2020; Li et al., 2021; Liu et al., 2022; Ma et al., 2021).

As the demand for clean and sustainable energy sources grows, enhancing the efficiency and output of PV systems becomes paramount (Baghel et al., 2023). tackle the intricate task of evaluating and optimizing the albedo (reflectivity) and tilt angle of photovoltaic panels to maximize their performance. By comprehensively examining how the reflective properties of surrounding surfaces and the orientation of panels impact energy generation, the research seeks to identify the most suitable albedo levels and tilt angles for different conditions. By addressing these variables, the article contributes to the ongoing efforts to boost the overall effectiveness and viability of solar PV systems, leading to improved energy capture, system productivity, and environmental benefits. On the other hand, there is a key challenge related to the integration of photovoltaic (PV) technology into building facades. As the integration of renewable energy sources into architectural designs gains momentum, there is a growing need to evaluate the performance of large-sized PV modules specifically designed for façade integration. In (Assoa et al., 2023), the authors address the intricate issue of how such modules perform under real-world conditions, considering factors like solar exposure, shading, and architectural aesthetics. By analyzing the performance of these specialized PV modules, the research seeks to shed light on their energy generation capabilities and overall efficiency when integrated into building facades. The findings of this study are crucial for architects, engineers, and policymakers striving to create sustainable and energy-efficient buildings by seamlessly incorporating solar technology into their designs, thus contributing to the ongoing progress in renewable energy adoption and sustainable urban development.

The study (Yang et al., 2023) decided to optimize the performance of PV modules and solar cells through the innovative application of a hybrid and efficient chimp algorithm. By employing this algorithmic approach, the research aims to fine-tune the parameters that significantly impact the energy conversion efficiency of PV systems, thus improving their overall power output. The study's findings hold significance for the renewable energy sector, offering insights into advanced optimization techniques that can be applied to maximize the energy yield of solar installations. This research contributes to the ongoing pursuit of efficient and effective solar energy utilization, paving the way for increased adoption of clean and sustainable power generation technologies.

Other studies (Soler-Castillo et al., 2023; Padilla et al., 2022; Toledo et al., 2023) address the intricate issue of modeling and simulating the dynamics of I-V (current-voltage) curves, which are fundamental in characterizing the behavior of solar cells under varying conditions. By developing an approach to simulate the complex dynamics of these curves, the research aims to enhance the predictability of PV system performance. The insights gained from these studies are invaluable for optimizing energy capture, forecasting power generation, and guiding system design and maintenance strategies.

PV technology presents a necessary review of various circuit topologies employed for I-V curve tracing, a technique essential for assessing the efficiency and health of PV systems. By analyzing the strengths and limitations of different tracer topologies, researchers aim to guide the development of more effective and accurate measurement techniques. Researchers contribute to the advancement of photovoltaic technology by offering insights into the instrumentation and methodologies required to better comprehend the behavior of solar cells, ultimately leading to improved system design, monitoring, and maintenance practices (Zhu and Xiao, 2020; Zhang et al., 2022; Olayiwola and Choi, 2023; Blakesley et al., 2020).

The challenge of developing I-V curve tracers is assumed by the necessity of offering portable and modern devices to improve the ways of evaluating PV performance. In (Casado et al., 2022) authors focused on the development and implementation of a novel I-V (current-voltage) curve tracer using Raspberry Pi, a versatile and affordable single-board computer. The main problem tackled is the need for a cost-effective and accessible method to trace I-V curves of PV modules, enabling a better understanding of their behavior under varying conditions. By utilizing Raspberry Pi as the core of the tracer, the research provides a practical solution for researchers, engineers, and enthusiasts to measure and analyze I-V curves in a user-friendly manner. This innovation has the potential to democratize the process of characterizing PV modules, contributing to the broader goals of advancing solar energy technology and facilitating its widespread adoption. On the other hand, the study (José Muñoz-Rodríguez et al., 2023) focuses on enhancing the performance analysis of rooftop PV systems by introducing new parameters derived from monitored data, in alignment with the guidelines provided by IEC 61724 standard. The primary challenge addressed is the need for more comprehensive and refined methods to assess the output and efficiency of rooftop PV installations. By developing novel parameters and metrics based on monitored operational data, the research aims to provide a more accurate and comprehensive understanding of system performance. This approach holds importance for stakeholders ranging from solar energy industry professionals to policymakers, enabling better decision-making, and systems optimization, and ultimately fostering the integration of rooftop photovoltaics as a viable and efficient renewable energy solution.

Several authors research about PV failures. In (Belhaouas et al., 2024), a study on PV module failures reveals various challenges and performance issues faced by photovoltaic systems. The analysis included six types of PV modules with different outdoor exposure durations under the Mediterranean climate. Most PV modules did not meet their expected yearly degradation rates (except for one type) with 17 years of outdoor exposure showing a very low rate compared to the expected rate. Most common failure modes include detached junction boxes due to poor adhesion as well as degradation in electrical performance.

Another studies (Nieto-Morone et al., 2024; Özkalay et al., 2024) proposed several innovative solutions for improving PV module performance and lifespan including, among others: utilizing advanced diagnostic tools such as electroluminescence imaging and infrared thermography for early detection of faults (e.g. cracks, hotspots, moisture-induced degradation); implementing stringent quality control measures throughout the manufacturing process; adopting international standards (IEC, ISO) and adapting them to local conditions; establishing national certification and training programs for PV installers and designers can ensure high-quality installation practices; and, developing circular supply chains for PV modules, including recycling,

refurbishment, and re-certification, can extend the lifespan of PV systems. This approach not only improves sustainability but also enhances the overall economic viability of solar energy.

Multiple authors have focused on measuring and adopting solar community methods. In (Ángel-Antonio Bayod-Rújula, 2014), the inefficiency and malfunction of traditional Maximum Power Point Tracking (MPPT) techniques in photovoltaic systems under rapid irradiance changes and partial shading conditions were addressed. The paper suggests a fresh MPPT method that incorporates photodiodes as irradiance sensors, which enables accurate measurement of shadow coverage, precise monitoring of light exposure levels, MPPT algorithm adjustment to prevent malfunctions; all leading to more efficient energy output optimization. This technique underwent theoretical examination with conventional strategies while displaying improved efficiency feasibility for practical applications. The authors introduce an efficient technique in (Kumar and Nayak, 2024) to identify and pinpoint faults occurring within PV arrays, utilizing the cumulative sum (CUSUM) of string current variations. This method relies solely on measuring individual string currents and can promptly detect a range of fault types - such as low mismatch or high resistance faults - with great precision within 5 ms. Moreover, it excels at accurately distinguishing between real faults versus non-fault situations like partial shading; thereby surpassing typical protective devices and other pre-existing techniques to signal when damage occurs.

This article presents an innovative development of a portable and fast characterizer of the performance of photovoltaic panels. The device allows for the acquisition of solar radiation, ambient temperature, electric current, and voltage generated by the solar panel to plot I-V and P-V curves. Additionally, a mobile application has been developed that enables the configuration and operation of the device over the internet through any mobile phone. The paper is structured in a way that first introduces the theoretical model for the characterization of photovoltaic panels, then describes the experimental device design along with the methodology, and finally presents the obtained results and conclusions.

2. Device implementation

Accurate measurements and efficient system management are crucial when developing our device to monitor photovoltaic panel performance. Therefore, it is essential to understand and control ambient conditions such as temperature. Temperature significantly impacts the efficiency of photovoltaic panels, making it necessary to measure both the ambient temperature and surface temperature of each panel with calibrated sensors. The semiconductor's thermal activity increases at higher temperatures which can reduce a panel's effectiveness in generating energy output. To overcome this challenge, implementing cooling mechanisms or selecting materials that have better thermal management properties becomes imperative for mitigating these effects on solar cells' overall efficacy.

Monitoring solar irradiance is crucial for accurately measuring the power output of photovoltaic panels. Pyranometers and photodiodes are capable of capturing the intensity levels of solar radiation falling on a panel, ensuring precise readings. To maintain accuracy in these measurements, diligent upkeep must be followed to avoid obstruction or interference with sensor function along with consistent calibration against reference standards. Proper placement techniques that eliminate turbulence should also be employed as they contribute to vital data accuracy while recording wind conditions.

To shield the equipment from environmental factors, it is advisable to incorporate weather-resistant sensors and protective housings. Additionally, monitoring of soiling on the surface of PV panels caused by dust and dirt should be done through visual inspections or soiling sensors as this could cause significant efficiency reduction. The upkeep of optimal panel performance necessitates periodic cleaning exercises alongside assessments for any signs of accumulating dirt.

To guarantee precision, the sensors necessitate a series of fundamental steps in their calibration process. The correct measurements for temperature sensors are achieved by calibrating them against an established standard thermometer amidst controlled circumstances. Similar to this method is how irradiance sensors operate via calibration using either STC-controlled conditions or other recognized standards as they're compared with reference pyranometers for accuracy verification purposes respectively. Finally, electrical calibration requires state-of-the-art multimeters and solid power sources functioning as references while assessing current-voltage sensing devices and power meters during testing processes conducted accordingly.

To maintain accuracy in the performance monitoring system, recalibration must be conducted regularly either as per manufacturer instructions or specified intervals. To account for variances in temperature, wind conditions and irradiance; environmental compensation algorithms can also be utilized to adjust measurements. Moreover, periodic validation of the entire system against a reference point or under standard conditions should be carried out to ensure that long-term precision is sustained without fail.

When deploying the monitoring device, it is crucial to merge all sensors into a coherent data acquisition infrastructure that ensures synchronized data logging and comprehensive performance analysis. To swiftly detect any issues in system performance, real-time data processing capacities are necessary; meanwhile, sturdy storage options for information along with advanced analytical tools make evaluating long-term changes simple while supporting predictive maintenance practices. Additionally, having an easily navigable user interface helps users interpret PV panel-related data without difficulty by providing clear graphical displays and remote access functionality through intuitive dashboards.

Developing a PV panel performance monitoring device that observes ambient conditions and follows a strict calibration process can yield precise, dependable, and practical data to improve the effectiveness and sustainability of photovoltaic systems.

If one tackles the surrounding circumstances and meticulously follows a calibration procedure, it is possible to create a monitoring gadget for PV panels that offers precise, trustworthy, and practical information. Such data can optimize both efficiency and durability of photovoltaic systems.

The performance measurements of photovoltaic panels can be notably affected by environmental conditions present at testing sites, where temperature, solar irradiance and dust levels have an essential impact on the precision and dependability of collected data.

Fluctuations in ambient and panel surface temperatures can impact the photovoltaic panels' efficiency. The effectiveness of these solar devices is generally reduced by higher temperatures due to increased internal resistance, resulting in lower power output. Conversely, cooler temperatures tend to boost their performance significantly; hence temperature sensors are vital tools for tracking fluctuations and adjusting relevant calculations correspondingly.

The performance of solar panels greatly depends on the amount and strength of sunlight they receive - known as Solar Irradiance. Accurate measurement and evaluation are crucial for gauging their efficacy under varying conditions caused by cloud cover, time of day or seasonal changes. Pyranometers and photodiodes measure irradiance levels but must be calibrated periodically to ensure precision in readings.

The accumulation of dust and dirt on photovoltaic panels can block sunlight, significantly lowering their efficiency. Maintaining optimal performance requires regular monitoring and cleaning. One may use visual inspections or soiling sensors to assess panel contamination levels.

To preserve the precision of sensors utilized for environmental monitoring, regular calibration is essential. This entails subjecting sensor readings to controlled conditions and comparing them against established benchmarks. Moreover, maintaining both the monitoring system and sensors on a routine basis guarantees reliable performance measurements are obtained.

Accurate and reliable performance measurements of photovoltaic

panels can be achieved by meticulously examining and adjusting for environmental factors. This enables an enhanced comprehension and enhancement of the longevity as well as productivity of these panels under real-life circumstances.

2.1. Theoretical model

Fig. 1 shows the circuit model of a photovoltaic solar cell. Iph current source represents the generated photocurrent, D diode represents the P/N connection, Rs represents the serial number of the resistive device, which is related to the strength of the material and electrical contact, Rsh represents the current consumption of the resistive parallel device and is related to the current consumption in the device volume ("Practical Handbook of Photovoltaics, 2023).

Photovoltaic cells are often presented in the form of cells connected in series to increase the output voltage to a desired value, and in parallel to increase the current that a device can provide depending on the power demand (Perez, 2023). Each solar cell behaves like a p/n rectifying diode in the dark and generates a photocurrent when exposed to light.

A mathematical model of the equivalent circuit of a solar photovoltaic cell is described below (Duru, 2006; Gow and Manning, 1999; Seguel).

Applying current Kirchhoff's laws, the current at the PV module terminals is:

$$Ipv = Iph - ID - IRsh \tag{1}$$

Where Ipv is the current generated by the system, Iph is the photocurrent generated, ID is the current flowing through the diode, and IRsh is the current flowing through the shunt resistor.

Eq. (2) is related to the photogenerated Iph current, which depends on standard irradiance and temperature (Seguel). G is the radiation of the existing station, T and Tr are the current station temperature and the reference temperature. Δi is the temperature coefficient of current and Isc is the short-circuit current of the battery at standard temperature.

$$Iph = \frac{G}{1000}[Isc + \Delta i(T - Tr)] \tag{2}$$

The ID diode saturation current can be found by the Shockley equation:

$$ID = Isat\left[\exp\left(\frac{VD}{Vt}\right)\right] - 1 \tag{3}$$

where Isat is the saturation current of the diode, VD is the diode voltage, Vt is the thermodynamic voltage of the diode, k is Boltzmann's constant, Tc is the temperature in the pn junction, and q is the electron charge value corresponding to the diode ideality factor.

Applying Kirchhoff's voltage law, we get:

$$VD = Vpv + Rs * Ipv \tag{4}$$

We replace VD and clear IRsh, we have:

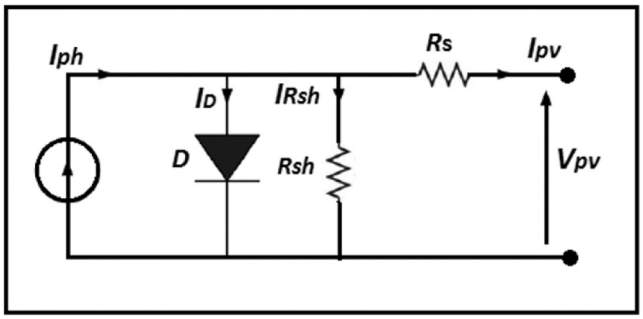

Fig. 1. Solar cell electrical model.

$$IRsh = \frac{Vpv + Rs * Ipv}{Rsh} \tag{5}$$

And:

$$Vt = \frac{A * K * Tc}{q} \tag{6}$$

The electrical characteristics of a PV module are given in terms of current and voltage output (Ipv – Vpv). so:

$$Ipv = Iph - Isat\left[\exp\left(\frac{VD}{Vt}\right) - 1\right] - \frac{Vpv + Rs * Ipv}{Rsh} \tag{7}$$

The Isat parameter must be evaluated as an open circuit, where:

$$Ipv = 0 \tag{8}$$

$$Vpv = Voc \tag{9}$$

Under these conditions, it is rewritten as follows:

$$0 = Iph - Isat\left[\exp\left(\frac{Voc}{Vt}\right) - 1\right] - \frac{Voc}{Rsh} \tag{10}$$

By simplification, we get:

$$Isat = \frac{Iph - \frac{Voc}{Rsh}}{\exp\left(\frac{Voc}{Vt}\right) - 1} \tag{11}$$

The reverse saturation current also depends on temperature (Kumar and Nayak, 2024):

$$Isat = Isatr * \left(\frac{Tc}{Tr}\right)^3 * \exp\left[\frac{q * Eq}{K * A}\right]\left[\frac{1}{Tr} - \frac{1}{TC}\right] \tag{12}$$

$$Tc = Ta + (0,2 * G) \tag{13}$$

where Isatr is the reference saturation current, Tc is the battery temperature, Tr is the reference temperature, Eq is the bandgap energy, q is the electron charge, and K is the Boltzmann constant. A corresponds to the ideality factor of the diode, Ta is the ambient temperature, and G is the solar radiation.

In short, we have:

$$Ipv = Icc \tag{14}$$

$$Vpv = 0 \tag{15}$$

Under these conditions, we have:

$$Icc = Iph - \frac{Iph - \frac{Voc}{Rsh}}{\exp\left(\frac{Voc}{Vt}\right) - 1} - \frac{Icc * Rs}{Rsh} \tag{16}$$

has been rewritten again:

$$Iph = \frac{Icc\left(1 - \frac{Rs}{Rsh}\right) - Voc\left(\frac{\exp\left(\frac{Icc*Rs}{Vt}\right) - 1}{\exp\left(\frac{Voc}{Vt}\right) - 1}\right)}{1 - \left(\frac{\exp\left(\frac{Icc*Rs}{Vt}\right) - 1}{\exp\left(\frac{Voc}{Vt}\right) - 1}\right)} \tag{17}$$

Then the Rs and Rsh resistances are ("Practical Handbook of Photovoltaics, 2023):

$$Rs = \left[1 - \frac{FF}{FFo}\right]\left(\frac{Voc, \mathrm{STC}}{Isc, \mathrm{STC}}\right) \tag{18}$$

$$Rsh = \frac{FFo(Vo + 0,7)}{(1 - \frac{FF}{FFo})Vo}\left(\frac{Voc, \mathrm{STC}}{Isc, \mathrm{STC}}\right) \tag{19}$$

where FF is the fill factor and FFo is the ideal fill factor (Green, 2023). If Rs=0, then:

$$FF = \frac{Pm}{Voc * Isc} = \frac{Vm * Im}{Voc * Isc} \tag{20}$$

$$FFo = \frac{Vo - Ln(Vo + 0,72)}{Vo}; with\ Vo = \frac{Voc}{KTc} \tag{21}$$

Substituting Eqs. (11) and (17) into Eq. (7), the following Eq. (22) y (23)are obtained:

$$Ipv = Iph - \frac{Iph - \frac{Voc}{Rsh}}{\exp\left(\frac{Voc}{Vt}\right) - 1}\left(\exp^{\frac{Vpv + Ipv * Rs}{VT}} - 1\right) - \frac{Vpv + Ipv * Rs}{Rsh} \tag{22}$$

$$\mathbf{Ipv} = \frac{\mathbf{Icc}\left(\mathbf{1} + \frac{\mathbf{Rs}}{\mathbf{Rsh}}\right) - \mathbf{Voc}\left(\frac{\exp\left(\frac{\mathbf{Icc*Rs}}{\mathbf{Vt}}\right) - 1}{\exp\left(\frac{\mathbf{Voc}}{\mathbf{Vt}}\right) - 1}\right)}{\mathbf{1} - \left(\frac{\exp\left(\frac{\mathbf{Icc*Rs}}{\mathbf{Vt}}\right) - 1}{\exp\left(\frac{\mathbf{Voc}}{\mathbf{Vt}}\right) - 1}\right)} - \left(\frac{\mathbf{Icc}\left(\mathbf{1} + \frac{\mathbf{Rs}}{\mathbf{Rsh}}\right) - \mathbf{Voc}\left(\frac{\exp\left(\frac{\mathbf{Icc*Rs}}{\mathbf{Vt}}\right) - 1}{\exp\left(\frac{\mathbf{Voc}}{\mathbf{Vt}}\right) - 1}\right)}{\left(\exp\left(\frac{\mathbf{Voc}}{\mathbf{Vt}}\right) - \mathbf{1}\right) - \left(\exp\left(\frac{\mathbf{Icc*Rs}}{\mathbf{Vt}}\right) - \mathbf{1}\right)}\right) - \frac{\mathbf{Voc}}{\left(\exp\left(\frac{\mathbf{Voc}}{\mathbf{Vt}}\right) - \mathbf{1}\right) * \mathbf{Rsh}}\left(\exp^{\frac{\mathrm{Vpv + Ipv * Rs}}{\mathrm{VT}}} - 1\right) - \frac{\mathrm{Vpv + Ipv * Rs}}{\mathrm{Rsh}} \tag{23}$$

The battery temperature (Tc) is determined based on the operating ambient temperature (Ta) and the NOCT (Battery Nominal Operating Temperature) specified by the manufacturer.

$$Tsc = Ta + \frac{NOCT - 20}{800}G(\mathrm{W/m2}) \tag{24}$$

The following equations correspond to the parallel and series impedance of PV modules, where Np is the number of cells connected in parallel, Ns is the number of cells connected in series, Rp is the resistance connected in parallel, and Rs is the series of resistors connected in parallel.

$$Rsht = \left(\frac{Np}{Ns}\right)Rp \tag{25}$$

$$Rst = \left(\frac{Ns}{Np}\right)Rs \tag{26}$$

2.2. Experimental design

2.2.1. Device requirements

The device is aimed at acquiring and processing signals. Additionally, the device will have a Platform as a Service architecture.

For the design of the device, the following considerations are taken into account:

- The device must be capable of characterizing panels of up to 250 watts.
- It should be able to respond to requests via the HTTP protocol.
- The power stage must be isolated from the control stage.
- Operating voltages on the microcontroller must not exceed 3.3 V.
- Protection and regulation elements must be considered.
- Signals should be filtered if necessary.
- The device should create an Access Point for characterization purposes.
- The device should be compact and have a protective casing.

For these purposes, an ESP32 microcontroller from Sparkfun has been selected. It features a WiFi module capable of connecting to mobile devices. It has 28 GPIO pins and also provides support for low-energy Bluetooth connections. The versatility of the ESP32 shines in IoT project execution. Its operating range is from 2.2 to 3.3 V, and it has low power consumption (less than 100 mA). There are 18 analog-to-digital converter (ADC) pins, 2 digital-to-analog converter (DAC) pins, and 3 SPI interfaces. The ESP32 microcontroller meets the industry-standard SDIO card specification Version 2.0 and allows a host controller to access the SoC, using de SDIO bus interface and protocol. Table 1 displays the basic specifications of the ESP32 microcontroller.

2.2.2. Sensors

- Current sensor

  The ACS712 current sensor provides cost-effective and precise solutions for detecting alternating current (AC) and direct current (DC) in the industry. The device consists of a linear Hall effect sensor with a copper conduction path located near the surface of the chip. The supply voltage is 5 V, and the output voltage is proportional to AC or DC currents. The ACS712 sensor has low noise in the analog signal and a sensitivity range of 66–185 mV/A. It can measure up to 20 A of input current from a load.
- Voltage sensor

  It's essentially a voltage divider consisting of two resistors in series, powered by 7.4 V, designed to measure voltage from 0 V up to 50 V. This voltage is scaled from 0 V to 3.3 V so that it can be sent to the ESP32 microcontroller.
- Temperature sensor

  The NTC 10 K sensor is an ideal temperature sensor for measuring ambient temperature. It comes with a stainless-steel housing and is waterproof. It provides a linear output proportional to temperature, starting at 0 volts at 0 degrees and a 10 mV output voltage change for

Table 1
Technical specifications of the ESP32 microcontroller.

Parameter	Description
Processor	Dual-core Tensilica LX6
Clock Frequency	Up to 250 MHz
SRAM	520 kB internal
GPIO	28
Operating Range	From 2.2 V to 3.3 V
DAC	2
Flash Memory	4MB
ADC	17–18
Aditional features	WiFi, Bluetooth, touch sensor, LI ion

every degree change, with a measurement range of −20–105 degrees Celsius.
- Irradiance sensor

The SP Lite2 is a solar radiation sensor primarily used for measurements in photovoltaic modules and can be used under various weather conditions. Its operating principle relies on a photodiode that generates an output voltage proportional to incoming radiation, with sensitivity varying with the cosine of the incidence angle of the radiation. This pyranometer meets the following international standards: EN 63000:2018 and EN 61326:2013. Table 2 shows the main technical specifications of the SPLite 2 sensor.

2.2.3. Signals conditioning

As a voltage regulator, we used a switching step-up module XL6009, which allows for increasing voltages in the range of 5 V to 35 V with a current load of 3 A. We also employed the XL4015 module, which is a switching step-down voltage regulator, enabling voltage reduction in the range of 1.25 V to 35 V with a current load of 5 A. For analog-to-digital conversion, we utilized the ADS1015 module, providing a 12-bit resolution at a rate of 3300 samples per second using the I2C bus. Additionally, its programmable gain amplifier allows configuration of up to 16x for signals that are too small.

The AD620 module is an instrumentation amplifier capable of amplifying signals in the microvolt/millivolt range with gains ranging from 1.5 to 1000 times the input signal. The AD620 module meets JEDEC standards MS-001 and MS-012-AA. As an energy storage system, we selected a 3500 mAh, 7.4 V LiPo battery with a module that allows for monitoring and measuring its charge level.

MOSFET transistors are ideal for high-frequency switching since they are not adversely affected at high speeds, which allowed us to determine a frequency of 1.25 KHz for the PWM signal to be implemented. We selected a P-type MOSFET transistor, specifically the IRFZ44N, with a maximum Drain-Source voltage of −100 V and a maximum drain current of −13 A. To control the switching of the MOSFET referenced by the panel and the 7.4 V battery, we use PWM generated by the ESP32, in order to bring the MOSFET into the cut-off and saturation regions with voltage variations. The output voltage of the microcontroller is referenced from 0 V to 3.3 V; however, to drive the MOSFET, a higher voltage is required. This is why it was necessary to implement an opto-coupler stage to increase the signal coming from the microcontroller and thus exceed the gate-source voltage (VGS) required for MOSFET switching. Fig. 2 shows the initial switching circuit for characterizing the solar panel.

This switching circuit features an IRFZ44N MOSFET that receives a 7.4 V PWM signal, allowing the MOSFET to enter the cut-off and saturation states without any issues. The load in this case is the same MOSFET, as it dissipates power when in saturation. Since it operates in switching mode, heat dissipation is much lower compared to when it is in the ohmic region. Nevertheless, a heatsink with forced ventilation is added to reduce the impact of high currents.

Located between the drain and source is the panel to be characterized, which is connected in series with a 20 A ACS712 current sensor. Since this sensor has a copper connector, it acts as a shunt resistor, stabilizing the system. In parallel with the panel and the current sensor, an RC branch is placed as a low-pass filter to reduce noise generated by

Table 2
Technical specifications of the SPLite 2 sensor.

Parameter	Description
Spectral range	400 nm – 1100 nm
Sensitivity (nominal)	72 uV/Wm^{-2}
Response time	Lower than 1 s
Maximum radiation	2000 Wm^{-2}
Directional error	±5 % for angles above 80 degrees

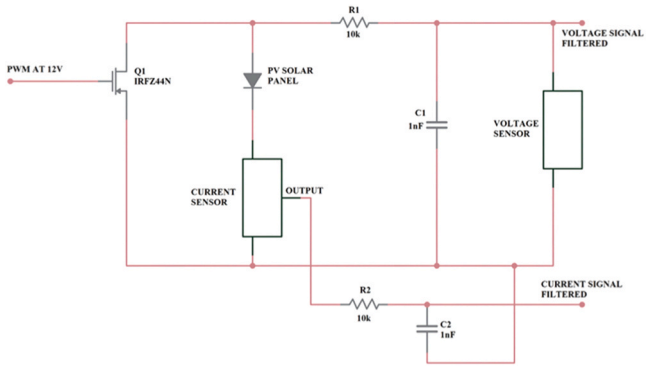

Fig. 2. Initial circuit to PV panel characterization.

switching and obtain a more accurate measurement. Similarly, there is a filter for the current signal.

Initially, this circuit does not yield very good results, so certain improvements are required. Fig. 3 shows the initial results of this circuit.

Fig. 3 displays the output variables (I and V) in their unconverted form, meaning their analog values are shown. In this case, the output is nearly linear, which could be attributed to the fact that the carrier signal (PWM) is not being filtered. It is necessary to improve the filtering as the carrier signal is at 1.25 KHz. Finally, a 4700μF capacitor is used to smooth and filter the carrier signal, but it was observed that the capacitor triggers a very high current peak when it enters a short circuit, which could potentially cause permanent damage to the MOSFET. To prevent this, current filtering is added, thus completing a second-order filter. Fig. 4 shows the electronic model created in Proteus and KiCad software for the second-order filter. Fig. 5a depicts the obtained I-V curve.

With the assistance of the second-order filter, the MOSFET no longer sustains damage, and the output signal closely matches the natural behavior of the PV panel. As the final outcome, the design of a PCB circuit is initiated.

2.2.4. Printed circuit board design

The ESP32 serves as the central device in the PCB design, where all input and output signals converge. Each signal has its respective filtering stage. Since the ESP32 has a maximum output of 3.3 V, it is opto-coupled to transmit the signal at 7.4 V, surpassing the required gate-source voltage (VGS) for proper switching. Additionally, this helps ensure that if the MOSFET tends to draw current due to parasitic capacitances, the current is supplied by the 7.4 V battery rather than the ESP32, preventing potential damage.

The ACS712 current module employs a resistor arrangement to

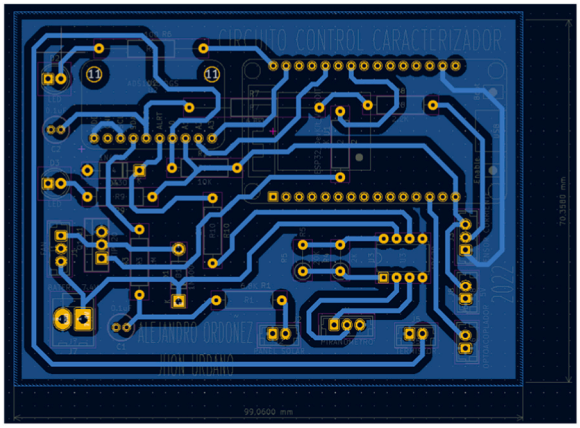

Fig. 3. PCB of the control circuit.

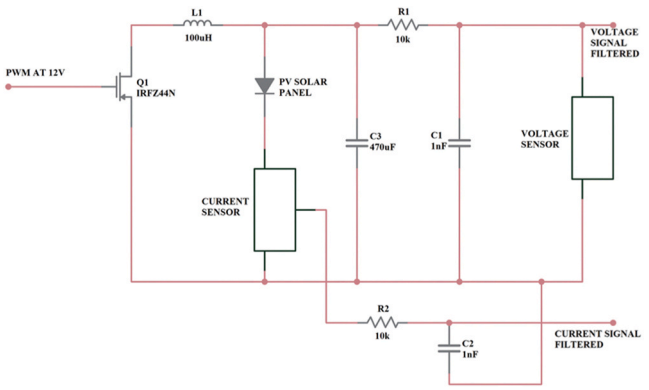

Fig. 4. Electronic circuit using the second-order filter.

calculate the current passing through the sensor within a voltage range of 0 V to 5 V. The voltage sensor utilizes a series circuit principle for voltage measurement. The resistances were calculated to establish a measurement window between 0 V to 5 V, which can be read by the ADS1015. The instrumentation amplifier module allows for the amplification of the radiation sensor's voltage. It was configured to amplify the signal within the 0 V to 5 V range to match the voltage levels of the ADS1015. Fig. 5b shows the printed board circuit and, Fig. 5c depicts the assembled sensors, connectors, and batteries.

2.2.5. Housing design

Since the device must be sturdy enough for regular use, it is necessary for it to have a casing that protects it from impacts, and dust, and isolates the circuit from human contact. This also ensures better component security, preventing wear on the cables or loss of components.

For the design, Autodesk Inventor 2022 software was chosen to create a 3D model that ensures space for each component. The model is intended to be user-friendly, so a small, easily transportable box-like structure was chosen as a reference. This design allows for easy manipulation of the system. Fig. 6 shows the implemented casing design.

2.2.6. Software design

The development of the software application for the device was carried out using a service-oriented architecture, which is a communications technique that has grown due to the constant evolution of device availability. A service is a piece of software that provides functionality to other pieces within or outside the system. The software components that consume or query these services are known as clients and can be anything from a web page to a mobile application or even another service that requires it to complete functionality.

A programming framework is a toolkit that assists the developer in executing projects in an agile manner, utilizing libraries and native APIs of each platform. Each framework manages its own structure with a specific language (Java, C#, Javascript, etc.). The framework utilized in this research was Cross-Platform, characterized by being a development approach where multiple platforms can be targeted from a common codebase through the use of different frameworks (Ionic, Flutter, Xamarin.Forms, React Native, etc.). Xamarin.Forms was the framework used for developing the application for the following platforms: Android, Linux, iOS, Windows 10, and WPF.

3. Device calibration

3.1. Current sensor calibration

The calibration of the ACS712 current sensor was performed using a 20 A source connected in parallel to the sensor. Approximately 100 samples were taken, varying the current provided by the source, which was reflected in voltage variations in the sensor. Using the ADS1015, the voltage value calculated by the module's library was obtained for the various points generated during the measurement, from which the representative equation of the found straight line was generated. Fig. 7

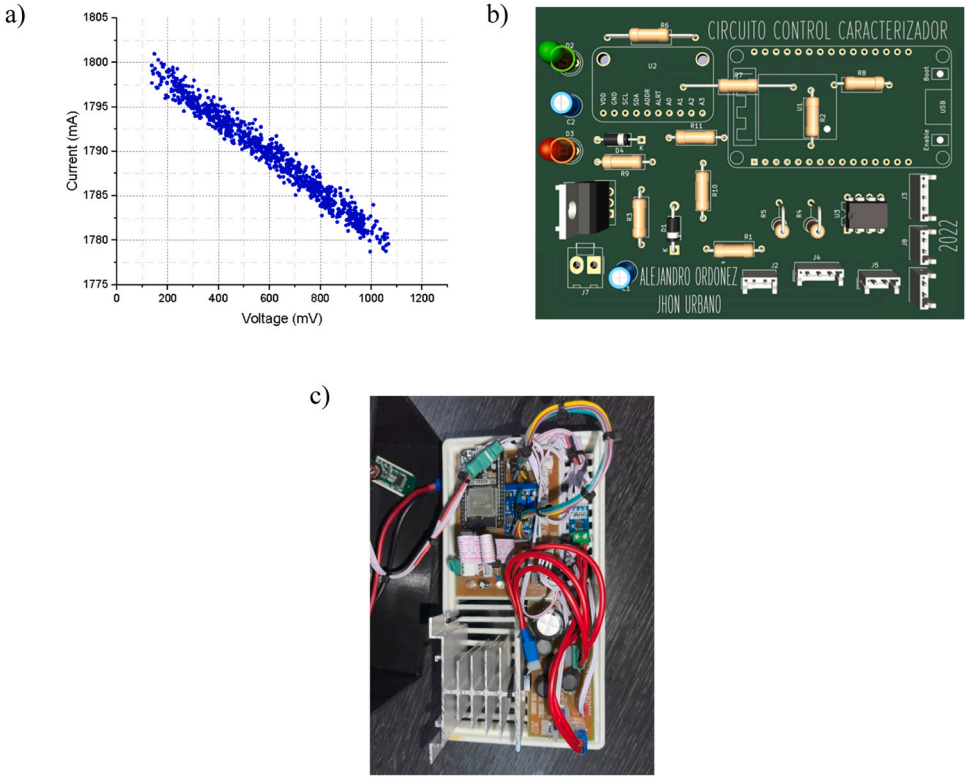

Fig. 5. (a) Initial results of the PV characterization, (b) 3D control circuit, and (c) Hardware of the assembled sensors, connectors, and batteries.

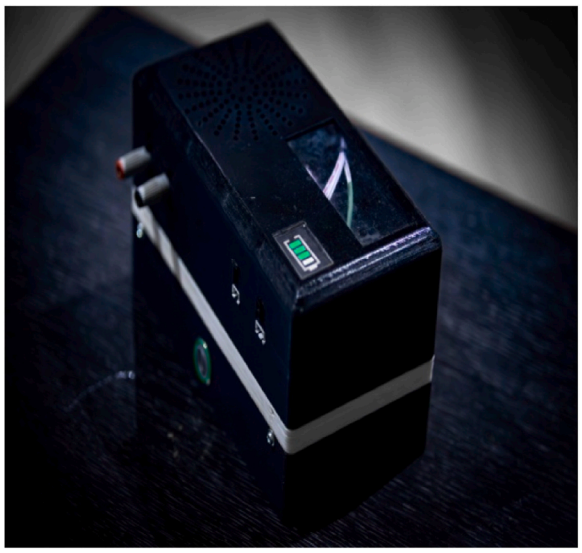

Fig. 6. Implemented housing design.

shows the calibration performed on the current sensor, using the 20 A source, and the calibration equation for the current sensor.

3.2. Voltage sensor calibration

A voltage source with a range of 0 V to 50 V was used for calibrating the voltage sensor. Approximately 116 samples were taken, varying the voltage provided by the source. These variations were reflected in voltage changes in the sensor. Using the AD620, the analog value of the various points generated during the measurement was obtained, and from this, the representative equation of the found straight line was generated.

3.3. Temperature sensor calibration

The temperature sensor used is a 10KOhm NTC thermistor. To determine the temperature value, there is an array of resistors that provides a reference, i.e., a fixed value to compare with to detect the voltage change. This change represents the temperature value in ohms. However, it is necessary to arrive at a temperature unit, which is described by the Steinhart-Hart equation.

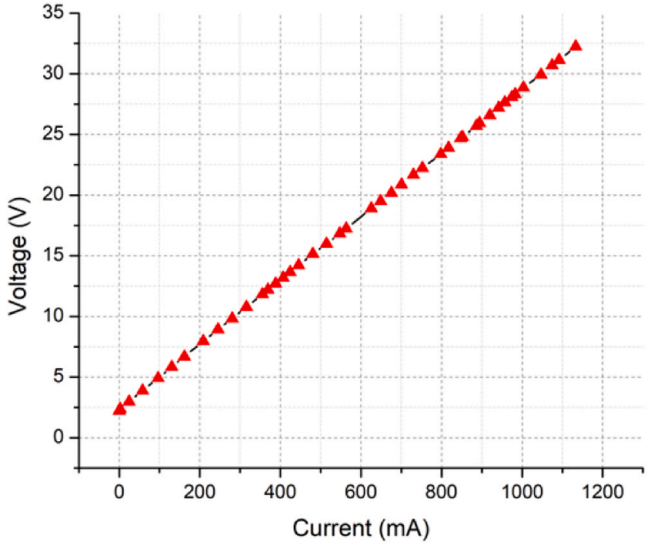

Fig. 7. Process calibration for the current sensor.

The Steinhart-Hart equation describes a transfer function of the ideal linear model, which is limited to a specific temperature range depending on the manufacturing and model of the thermistor. The transfer function helps eliminate this limitation.

3.4. Solar irradiance sensor calibration

The SP Lite2 pyranometer was calibrated using a certified reference Eppley Serie: 35136f3. Fig. 8(a-b) shows the electronic calibration process and depicts the certified pyranometer and the SP Lite2.

The pyranometer calibration process was carried out under real solar radiation conditions. Fifty samples were taken over a span of 4 hours to correlate solar radiation data at different times of the day. Using a multimeter, the analog voltage value of various points generated during the measurement was obtained, and from this, the representative equation of the found straight line was generated. A measurement error of 5.1 % was obtained between the standard pyranometer and the SP Lite2 pyranometer.

3.5. Comparative cost analysis

1. Hardware Costs

- Microcontrollers/SoCs: The choice of microcontroller or System on Chip (SoC) affects the overall cost. Popular choices include Arduino, Raspberry Pi, and ESP32.

o Arduino Uno: $25
o Raspberry Pi 4: $35
o ESP32 (selected): $6

- Sensors: To monitor photovoltaic panels, various sensors are needed for measuring voltage, current, temperature, and irradiance.

o Voltage and Current Sensors: $40 - $80 per unit
o Voltage and Current Sensors (selected): $10 - $30 per unit
o Temperature Sensors: $60 per unit
o Temperature Sensor (selected): $10 per unit
o Irradiance Sensors: $700 - $1000 per unit
o SP Lite 2 Irradiance sensor (selected): $500

- Communication Modules: Modules for Wi-Fi, Bluetooth, or cellular connectivity.

o Wi-Fi Module (ESP8266 selected): $5
o Cellular Module (SIM800L): $15

2. Software Development Costs

- App Development: The cost of developing a mobile application varies based on complexity and platform (iOS, Android).

o Simple App (selected): $200 - $500
o Advanced App: $20,000 - $50,000

- Firmware Development: Custom firmware for the microcontroller/SoC.

o Basic Firmware (selected): Free
o Advanced Firmware: $5000 - $10,000

3. Cloud Services and Data Management

- Cloud Hosting: Costs for hosting data and running cloud-based analytics.

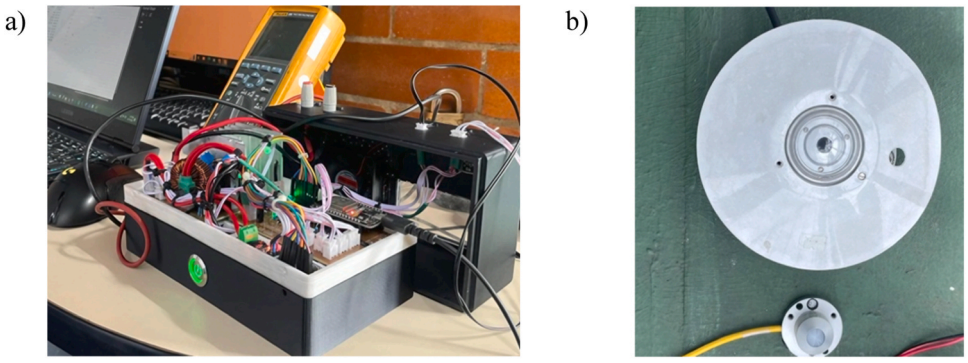

Fig. 8. (a) Electronic calibration process, and (b) Certified pyranometer (up) and SP Lite2 (down).

- o Basic Hosting (AWS Free Tier): $50 - $100 per month
- o Advanced Hosting: $100 - $700 per month

- Data Analytics Tools: Tools and services for data processing and analysis.

- o Basic Tools (selected): Free
- o Advanced Tools (AWS IoT Analytics): $5 - $50 per month

- No cloud services (Local data management and storage – selected): Free

4. Testing and Quality Assurance

- Hardware Testing: Cost for testing hardware components and the integrated system.

- o Basic Testing (selected): $1000
- o Advanced Testing: $4000

- Software Testing: Ensuring the app and firmware function correctly.

- o Basic Testing (selected): $200
- o Advanced Testing: $5000

5. Labor Costs

- Development Team: Cost for a team of developers, engineers, and designers.

- o Small Team (2 students in Master thesis - selected): Free
- o Large Team (10–15 members): $200,000 - $500,000 per year

Total Estimated Costs

- Proposed device: $1000 - $1200
- Advanced System: $275,000 - $630,000

Table 3 shows a comparative analysis of the proposed device with existing technologies.

- Device A (Solmetric PV Analyzer): This device offers comprehensive measurement capabilities including IV curve tracing, irradiance, temperature, voltage, and current. It is highly accurate and suitable for professional use with detailed data logging and advanced diagnostics. However, it is expensive and requires professional installation and regular calibration.
- Device B (Fluke IRR1-SOL Solar Irradiance Meter): This is a moderately priced, handheld device primarily focused on measuring solar irradiance and temperature. It is easy to use and portable, making it suitable for quick assessments. However, it lacks data logging capabilities and real-time monitoring, and offers moderate accuracy.
- Device C (SMA Sunny SensorBox): This device provides high accuracy measurements of solar irradiance, temperature, and wind speed with integrated logging and remote data access. It is designed for permanent installation with weather-resistant features, making it highly durable. It is also expensive and requires professional setup and regular calibration.
- Proposed Device: This proposed solution aims to provide essential monitoring capabilities such as solar irradiance, temperature, current, and voltage at a significantly lower cost. It is designed for easy, DIY installation and offers basic data logging with potential

Table 3
Comparative cost analysis between 3 devices and our proposed device.

Parameter	Device A: Solmetric PV Analyzer	Device B: Fluke IRR1-SOL Solar Irradiance Meter	Device C: SMA Sunny SensorBox	Proposed Device
Measurement Capabilities	IV curve tracing, irradiance, temperature, voltage, and current	Solar irradiance, temperature, tilt angle	Solar irradiance, temperature, wind speed	Solar irradiance, temperature, current, voltage
Cost	High ($4000+)	Moderate ($2000-$3000)	High ($4000+)	Low ($1000)
Ease of Installation	Moderate (requires professional installation)	Easy (handheld device)	Moderate (requires setup and configuration)	Easy (DIY setup possible)
Accuracy	High	Moderate to High	High	Moderate
Data Logging	Yes (detailed logging with software support)	No (manual recording)	Yes (integrated logging and remote access)	Yes (basic logging, potential for integration with software)
Real-Time Monitoring	Yes	No	Yes	Yes
Durability	High (robust, designed for field use)	Moderate	High (weather-resistant)	Moderate (depends on component quality)
Calibration Required	Yes (regular calibration needed)	Minimal	Yes	Yes (regular calibration for accuracy)
Additional Features	Advanced diagnostics, remote access	Simple to use, portable	Weather monitoring, remote data access	Customizable based on components

integration with software for enhanced features. While it may not match the high accuracy and durability of the more expensive devices, it provides an affordable and customizable option for widespread adoption.

The proposed device, leveraging inexpensive components, strikes a balance between cost-effectiveness and essential functionality, making it a viable option for broader deployment in cost-sensitive markets.

4. Results and discussion

Experimental measurements of the device's performance were conducted at two different geographic locations and for two different types of photovoltaic panels in order to evaluate the device's performance under real operating conditions.

4.1. Experimental measurements at Bogotá, Colombia

In Universidad Jorge Tadeo Lozano (located at 4.068496, −74.04125) at Bogotá on which date and hour, Colombia was conducted the first experimental measurements. Fig. 9 shows the photovoltaic system installed on the roof of Engineering Researching Building of Universidad Jorge Tadeo Lozano, in which the portable device was connected.

Table 4 shows the technical data of the PV panel Trina Solar, ref. TSM 250PA05.08.

Samples were taken at different times of the day to guarantee the plotting of curves in different radiations. The goal is to reach currents in the panel that are measurable by the sensor. Fig. 10 shows an example of the graphical interface of the application on the cell phone with the results of Power-Voltage (PV) and Current-Voltage (I-V) curves.

The climate classification for Bogotá is Cfb (Temperate Oceanic), meaning cold to mild winters and cool summers. Precipitation is well distributed throughout the year. The low temperatures in the Colombian capital are due to the passage of some "eastern waves" through central Colombia. These climatic events influence atmospheric conditions and create a colder and rainier conditions in the city. This affects Bogotá's solar radiation, registering values of around 3.8 HSS-4 HSS. Temperatures in Bogotá can average 13.5°C, with warm hours during the dry season that can exceed 20°C. During this same period, due to increased surface outgoing longwave radiation enhanced by the absence of clouds, frosts can occur (temperatures below 0°C), especially in rural areas.

Results in Fig. 10a show an efficiency of 7.418 % for the conversion of solar irradiance to electricity by the PV panel with 503 W/m^2 of solar irradiance and 16.2 ºC of temperature. Thanks to the app development, the device can save the data for any measurement for export the information for further analysis. Fig. 10b shows the I-V curve obtained with data exported from the monitoring app. In this case, solar irradiance was about 250 W/m^2, affecting directly the produced power: short circuit current registered about 1.56 A and open circuit voltage 12.6 V. Dispersed data are visible in Fig. 10b as a consequence of the slow irradiance level.

Fig. 9. Photovoltaic system at Universidad Jorge Tadeo Lozano, Bogotá, Colombia.

Table 4
Technical specifications of the PV panel Trina Solar.

Parameter	Description
P_{max}	250 W
V_{mp}	30.3 V
I_{mp}	8.27 A
V_{oc}	37.6 V
I_{sc}	8.85 A
Max. system voltage	600 V DC
Bypass diode	15 A
Series breaker	15 A
Fire resistance	C class

4.2. Experimental measurements at Puerto Carreño, Colombia

In Universidad del Rosario experimental photovoltaic system (located at 6.83486°N; −67.483784E) at Puerto Carreño, (Colombia) was conducted the second experimental measurements. Fig. 11 shows the photovoltaic system installed on the floor of the experimental area of Universidad del Rosario, to which the portable device was connected.

Table 5 shows the technical data of the photovoltaic panel Talesun, ref. TP6F72M-405.

The climate of Puerto Carreño is tropical, with a rainy season from April to November and a dry season from December to March. From June to August, the rains are very abundant, at a monsoonal level, although they decrease in El Niño years.

Temperatures are high throughout the year, but especially from January to April, before the rains, when they can reach 38/39°C. From June to August, during the rainy season, temperatures decrease a bit, especially during the day, but humidity reaches its peak values for the year.

The city is located in the far east of Colombia, on the border with Venezuela, at 6 degrees north latitude, at the confluence of the Orinoco and Meta rivers. Fig. 12a shows the I-V curve obtained with data exported from the monitoring app for a solar irradiance of 639.2 W/m^2.

In Fig. 12a, results indicate a short circuit current of about 3.16 A with an open circuit voltage of about 35 V. PV panel degradation and the high environmental temperature could be responsible for the value of registered open circuit voltage. Fig. 12b shows the I-V curve obtained with data exported from the monitoring app for a solar irradiance of 168.2 W/m^2. As it shows, for small solar irradiance levels, the PV panel isn't able to perform its nominal power. Little short currents data are plotted for temperature levels since 15 °C. Also, with this small irradiance level, the current sensor presents problems in acquiring data at the beginning of the experimental test. The short circuit current reported for 168.2 W/m^2 was 1.1 A while the open circuit voltage dropped to 32.5 V.

4.3. Future enhancements

The integration of IoT capabilities enables the device to establish communication with other intelligent devices within a solar power system, leading to an enhancement in overall system management and efficiency. To enhance predictive maintenance further, implementation of machine learning algorithms could identify patterns that predict potential failures before they occur. In depth analytics on panel performance includes assessing degradation rates, environmental impacts and efficiency trends resulting in more profound insights for optimizing PV systems. Allowing users to customize their monitoring dashboards will increase accessibility while integrating sensors measuring atmospheric pressure, air quality and UV index results is essential in understanding

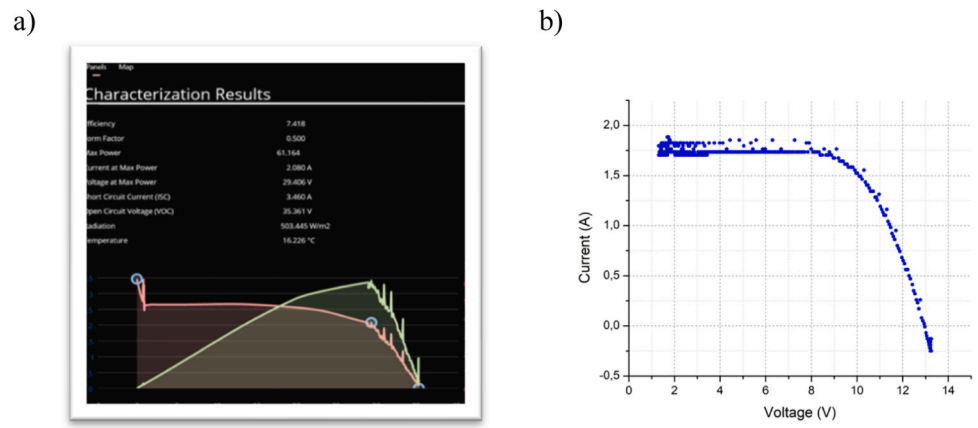

Fig. 10. (a) Mobile app interface showing I-V results and (b) I-V curve obtained for 650 W/m^2 irradiance.

Fig. 11. Photovoltaic system at Universidad del Rosario, Puerto Carreño Colombia.

Table 5
Technical data of the photovoltaic panel Talesun.

Parameter	Description
Pmax	405 W
Power tolerance	+3 %
Voc	49.3 V
Isc	10.5 A
Vmax	1000VDC
Temp.	45°C
Dimensions	2008*1002*35 mm
Application class	Class A
Weight	22.5 kg

how conditions affect PV panel effectiveness.

To maintain optimal efficiency of photovoltaic panels with minimal manual intervention, it is beneficial to develop automatic cleaning mechanisms that are triggered by the monitoring system when high levels of dust or soiling are detected. The accuracy and reliability of solar radiation measurements can be improved by utilizing more precise irradiance sensors with lower error margins. Temperature readings critical for assessing thermal impacts on PV efficiency will become even more accurate through employing temperature sensors with higher resolution and faster response times that withstand harsh environmental conditions ensuring long-term reliability while reducing maintenance obligations. By implementing self-calibrating technologies in sensors, measurement accuracy over extended periods will not require constant recalibration. Real-time monitoring processing speed up due to edge computing capabilities which reduce latency along development locations recognized resistant algorithms facilitate efficient storage transmission useful for continuous performance evaluation at impressive rates.

5. Conclusions

With the development of new microcontrollers and the advent of new technologies enabling electronics miniaturization, a device was created with a convenient, user-friendly design capable of immediately characterizing photovoltaic panels. This device competes with identical technologies available in the market that are more expensive and challenging for users to handle. The innovative factor of the device is linked to the development of the mobile application, allowing data visualization from any operating system.

One of the significant benefits of using a smartphone as a datalogger and data visualizer is the ability to work offline. This means that if you are working in an area with no coverage, you can still characterize photovoltaic panels and later synchronize the data with a server. This feature enables work in remote areas.

The collected data, when synchronized with a server, becomes accessible from anywhere and allows analysis using data analytics algorithms and Machine Learning. This enables the creation of predictive models and the detection of deficiencies in the system by identifying individual components such as end-of-life, poor positioning, etc.

The compact nature of the device allows for expansion in future versions with new functionalities, such as characterization of electrical production systems or improving signals with electronics focused on signal processing to achieve certification of quality according to established standards. Additionally, the device's protection, regarding its casing, can be certified to withstand IP55 standards (NEMA Enclosures, 2024) or higher.

Assessing the degradation and performance of PV modules accurately is crucial, which is where our developed device comes in handy. By offering real-time data along with diagnostic capabilities, this monitor helps detect potential issues like cracks or short circuits that affect efficiency and longevity of photovoltaic systems under fluctuating environmental conditions. As a result, it leads to better maintenance strategies while optimizing reliability & efficacy for solar installations over time.

By utilizing low-cost components like microcontrollers and DSPs, our development of a photovoltaic performance monitor has revealed valuable economic benefits. This approach significantly increases the cost-effectiveness and accessibility of PV systems by reducing the overall expense required for monitoring. As a result, this technology can be more widely deployed - particularly in markets where costs are critical-which may then reduce solar power's levelized cost (LCOE) as well as

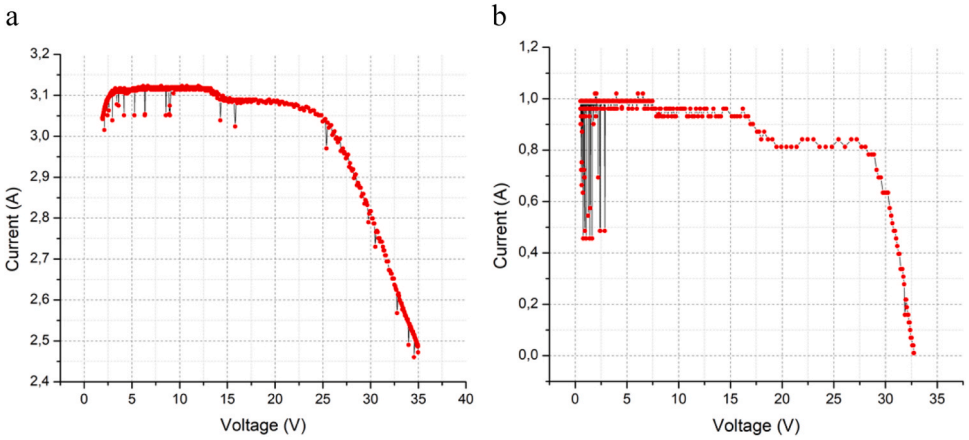

Fig. 12. I-V curve for Talesun PV panel at Puerto Carreño, Colombia: (a) 639.2 W/m^2 and (b) 168.2 W/m^2.

improve the viability of solar energy projects economically. What's more, these inexpensive monitoring solutions could help optimize module efficiency while extending their life cycle; thus decreasing maintenance expenses subsequently resulting in better return on investment for organizations that leverage them within their installations powered by Solar Energy Technology.

CRediT authorship contribution statement

O. Garcia: Supervision, Resources, Methodology, Investigation, Formal analysis. **B Quesada:** Writing – original draft, Validation, Supervision, Project administration, Funding acquisition. **A. Aristizábal:** Writing – review & editing, Writing – original draft, Visualization, Validation, Supervision, Methodology, Investigation. **Fredy Mesa:** Writing – review & editing, Writing – original draft, Validation, Supervision, Project administration, Investigation. **J. Urbano:** Software, Methodology, Investigation, Formal analysis, Data curation, Conceptualization. **S. Zapata:** Validation, Methodology, Investigation, Funding acquisition, Formal analysis, Data curation. **M. Castañeda:** Validation, Supervision, Software, Resources, Investigation. **A. Ordoñez:** Software, Methodology, Formal analysis, Data curation, Conceptualization.

Declaration of Competing Interest

The authors declare that they have no known competing financial interests or personal relationships that could have appeared to influence the work reported in this paper.

Data Availability

No data was used for the research described in the article.

Acknowledgments

The authors thank the project "Design and Implementation of a Portable Device for Evaluating the Performance of Photovoltaic Panels" between the University of Rosario, the Jorge Tadeo Lozano University, and Fundación Universitaria Los Libertadores, funded by the Colombian-French Researchers Association (COLIFRI) in the framework of the FSPI project "Ecosystem of Renewable Energies in Puerto Carreño".

References

Ángel-Antonio Bayod-Rújula, 2014. José-Antonio Cebollero-Abián, A novel MPPT method for PV systems with irradiance measurement. ISSN 0038-092X Sol. Energy Volume 109, 95–104. https://doi.org/10.1016/j.solener.2014.08.017.

Assoa, Y.B., Valencia-Caballero, D., Rico, E., Del Caño, T., Furtado, J.V., 2023. Performance of a large size photovoltaic module for façade integration. Renew. Energy vol. 211, 903–917. https://doi.org/10.1016/j.renene.2023.04.087.

Baghel, N., Manjunath, K., Kumar, A., 2023. Performance evaluation and optimization of albedo and tilt angle for solar photovoltaic system. Comput. Electr. Eng. vol. 110, 108849 https://doi.org/10.1016/j.compeleceng.2023.108849.

Belhaouas, N., Hafdaoui, H., Hadjrioua, F., Assem, H., Madjoudj, N., Chahtou, A., Mehareb, F., 2024. Failures and performance of different aged PV modules operated under northern Algerian climate conditions: Analysis, assessment, and recommended solutions. ISSN 1350-6307 Eng. Fail. Anal. Volume 163 (Part A). https://doi.org/10.1016/j.engfailanal.2024.108504.

Blakesley, J.C., Castro, F.A., Koutsourakis, G., Laudani, A., Lozito, G.M., Riganti Fulginei, F., 2020. Towards non-destructive individual cell I-V characteristic curve extraction from photovoltaic module measurements. Sol. Energy vol. 202, 342–357. https://doi.org/10.1016/j.solener.2020.03.082.

Casado, P., Blanes, J.M., Torres, C., Orts, C., Marroquí, D., Garrigós, A., 2022. Raspberry Pi based photovoltaic I-V curve tracer. HardwareX vol. 11, e00262. https://doi.org/10.1016/j.ohx.2022.e00262.

Chen, Z., Lin, Y., Wu, L., Cheng, S., Lin, P., 2020. Development of a capacitor charging based quick I-V curve tracer with automatic parameter extraction for photovoltaic arrays. Energy Convers. Manag. vol. 226, 113521 https://doi.org/10.1016/j.enconman.2020.113521.

Duru, H.T., 2006. A maximum power tracking algorithm based on Impp=f(Pmax) function for matching passive and active loads to a photovoltaic generator. Sol. Energy vol. 80 (7), 812–822. https://doi.org/10.1016/j.solener.2005.05.016.

Gow, J.A., Manning, C.D., 1999. Development of a photovoltaic array model for use in power-electronics simulation studies. IEE Proc. - Electr. Power Appl. vol. 146 (2), 193–200. https://doi.org/10.1049/ip-epa:19990116.

M.A. Green, "Solar cells: operating principles, technology, and system applications," Jan. 1982, Accessed: Sep. 02, 2023. [Online]. Available: ⟨https://www.osti.gov/biblio/6051511⟩.

Hosseini, A., Mirhosseini, M., Dashti, R., 2023. Analytical study of the effects of dust on photovoltaic module performance in Tehran, capital of Iran. J. Taiwan Inst. Chem. Eng. vol. 148, 104752 https://doi.org/10.1016/j.jtice.2023.104752.

Jathar, L.D., et al., 2023. Comprehensive review of environmental factors influencing the performance of photovoltaic panels: Concern over emissions at various phases throughout the lifecycle. Environ. Pollut. vol. 326, 121474 https://doi.org/10.1016/j.envpol.2023.121474.

José Muñoz-Rodríguez, F., Snytko, A., De La Casa Hernández, J., Rus-Casas, C., Jiménez-Castillo, G., 2023. Rooftop photovoltaic systems. New parameters for the performance analysis from monitored data based on IEC 61724. Energy Build. vol. 295, 113280 https://doi.org/10.1016/j.enbuild.2023.113280.

Kumar, Shubham, Nayak, Paresh Kumar, 2024. An effective method for detection and location estimation of faults in large-scale solar PV arrays. ISSN 0038-092X Sol. Energy Volume 277. https://doi.org/10.1016/j.solener.2024.112727.

Li, B., Delpha, C., Migan-Dubois, A., Diallo, D., 2021. Fault diagnosis of photovoltaic panels using full I–V characteristics and machine learning techniques. Energy Convers. Manag. vol. 248, 114785 https://doi.org/10.1016/j.enconman.2021.114785.

Li, B., Migan-Dubois, A., Delpha, C., Diallo, D., 2021. Evaluation and improvement of IEC 60891 correction methods for I-V curves of defective photovoltaic panels. Sol. Energy vol. 216, 225–237. https://doi.org/10.1016/j.solener.2021.01.010.

Liu, Y., et al., 2021. Fault diagnosis approach for photovoltaic array based on the stacked auto-encoder and clustering with I-V curves. Energy Convers. Manag. vol. 245, 114603 https://doi.org/10.1016/j.enconman.2021.114603.

Liu, Y., et al., 2022. Intelligent fault diagnosis of photovoltaic array based on variable predictive models and I–V curves. Sol. Energy vol. 237, 340–351. https://doi.org/10.1016/j.solener.2022.03.062.

Ma, M., Wang, H., Xiang, N., Yun, P., Wang, H., 2021. Fault diagnosis of PID in crystalline silicon photovoltaic modules through I-V curve. Microelectron. Reliab. vol. 126, 114236 https://doi.org/10.1016/j.microrel.2021.114236.

Ma, M., Zhang, Z., Xie, Z., Yun, P., Zhang, X., Li, F., 2020. Fault diagnosis of cracks in crystalline silicon photovoltaic modules through I-V curve. Microelectron. Reliab. vol. 114, 113848 https://doi.org/10.1016/j.microrel.2020.113848.

NEMA Enclosures, "IP55 Enclosures," Accessed: Jul. 13, 2024. [Online]. Available: ⟨https://www.nemaenclosures.com/enclosure-ratings/ip-enclosures/ip55-enclosures.html⟩.

Nieto-Morone, M.B., Rosillo, F.G., Muñoz-García, M.A., Alonso-García, M.C., 2024. Enhancing photovoltaic module sustainability: Defect analysis on partially repaired modules from Spanish PV plants. ISSN 0959-6526 J. Clean. Prod. Volume 461. https://doi.org/10.1016/j.jclepro.2024.142575.

Olayiwola, T.N., Choi, S.-J., 2023. Superellipse model: An accurate and easy-to-fit empirical model for photovoltaic panels. Sol. Energy vol. 262, 111749. https://doi.org/10.1016/j.solener.2023.05.026.

Özkalay, Ebrar, Virtuani, Alessandro, Eder, Gabriele, Voronko, Yuliya, Bonomo, Pierluigi, Caccivio, Mauro, Ballif, Christophe, Friesen, Gabi, 2024. Correlating long-term performance and aging behaviour of building integrated PV modules. ISSN 0378-7788 Energy Build. Volume 316. https://doi.org/10.1016/j.enbuild.2024.114252.

Padilla, A., Londoño, C., Jaramillo, F., Tovar, I., Cano, J.B., Velilla, E., 2022. Photovoltaic performance assess by correcting the I-V curves in outdoor tests. Sol. Energy vol. 237, 11–18. https://doi.org/10.1016/j.solener.2022.03.064.

A.J.Q. Perez, "Prototipo fotovoltaico con seguimiento del Sol para procesos electroquímicos", Accessed: Sep. 02, 2023. [Online]. Available: ⟨https://www.academia.edu/29415500/Prototipo_fotovoltaico_con_seguimiento_del_Sol_para_procesos_electroqu%C3%ADmicos⟩.

Piccoli Junior, L.A., De Oliveira, F.S., Gasparin, F.P., Krenzinger, A., 2023. Design and characterization of a continuous solar simulator for photovoltaic modules with automatic I-V curve acquisition system. Sol. Energy vol. 256, 55–66. https://doi.org/10.1016/j.solener.2023.03.057.

Practical Handbook of Photovoltaics - 1st Edition. ⟨https://shop.elsevier.com/books/practical-handbook-of-photovoltaics/mcevoy/978-1-85617-390-2⟩ (Accessed Sep. 02, 2023).

Seguel., J.I.L., Aug. 2009. "Projeto de um sistema fotovoltaico autônomo de suprimento de energia usando técnica MPPT e controle digital".

Soler-Castillo, Y., Sahni, M., Leon-Castro, E., 2023. Performance predictability of photovoltaic systems: An approach to simulate the I–V curve dynamics. Energy Rep. vol. 9, 234–269. https://doi.org/10.1016/j.egyr.2023.03.075.

Toledo, F.J., Galiano, V., Blanes, J.M., Herranz, V., Batzelis, E., 2023. Photovoltaic single-diode model parametrization. An application to the calculus of the Euclidean distance to an I – V curve,". Math. Comput. Simul., S0378475423000058 https://doi.org/10.1016/j.matcom.2023.01.005.

Yang, C., Su, C., Hu, H., Habibi, M., Safarpour, H., Amine Khadimallah, M., 2023. Performance optimization of photovoltaic and solar cells via a hybrid and efficient chimp algorithm. Sol. Energy vol. 253, 343–359. https://doi.org/10.1016/j.solener.2023.02.036.

Zhang, Z., Ma, M., Ma, W., Zhang, R., Wang, J., 2022. A data-driven photovoltaic string current mismatch fault diagnosis method based on I-V curve. Microelectron. Reliab. vol. 138, 114705 https://doi.org/10.1016/j.microrel.2022.114705.

Zhu, Y., Xiao, W., 2020. A comprehensive review of topologies for photovoltaic I–V curve tracer. Sol. Energy vol. 196, 346–357. https://doi.org/10.1016/j.solener.2019.12.020.